Remote Sensing Applications: Society and Environment 36 (2024) 101306

Contents lists available at ScienceDirect

Remote Sensing Applications: Society and Environment

journal homepage: www.elsevier.com/locate/rsase

# Using semi-automated classification algorithms in the context of an ecosystem service assessment applied to a temperate atlantic estuary

F. Afonso [a, *], C. Ponte Lira [b], M.C. Austen [c], S. Broszeit [d], R. Melo [a], R. Nogueira Mendes [a], R. Salgado [f], A.C. Brito [a, e]

[a] MARE – Marine and Environmental Sciences Centre, ARNET - Aquatic Research Network, Faculdade de Ciências da Universidade de Lisboa, Campo Grande, 1749-016, Lisboa, Portugal
[b] Instituto Dom Luiz, Faculdade de Ciências da Universidade de Lisboa, Portugal
[c] School of Biological and Marine Sciences, University of Plymouth, UK
[d] Plymouth Marine Laboratory, UK
[e] Departamento de Biologia Vegetal, Faculdade de Ciências da Universidade de Lisboa, Campo Grande 016, 1749-016, Lisboa, Portugal
[f] MARE, Escola Superior de Tecnologia de Setúbal, Instituto Politécnico de Setúbal, Campus do IPS, Estefanilha, 2910-761, Setúbal, Portugal

ARTICLE INFO

*Keywords:*
Habitat mapping
Remote sensing
Planet scope imagery
Support vector machines
Wetlands

ABSTRACT

The growing anthropogenic pressure near estuarine areas is evidence of the relevance of these systems to human well-being, especially because of their delivery of essential ecosystem services and benefits. Estuaries are composed of a rich large selection of habitats frequently organised in complex patterns. Mapping and further understanding of these habitats can contribute significantly to environmental management and conservation. The main goal of this study was to integrate different data sources to perform a supervised image classification, using remote-sensing products with different spatial resolutions and features. It was focused on the Sado Estuary, located on the Portuguese Atlantic coast. Considering the limitation of using free satellite images to map estuary habitats (i.e. limited spectral range and spatial resolution), this study uses a semi-automated supervised and pixel-based classification to overcome some of the derived classification problems. Support Vector Machine classifier was used to map the estuary for future evaluation of ecosystem services provided by each habitat. High-resolution remote sensing data (i.e., Planet Scope satellite images, aerial photographs) with different spectral and spatial features (3 m and 20 cm resolution, respectively) were used with ground truthing data to train the classifier and validate the derived maps. The first step of the classification identified broader classes of habitats in the satellite images based on visual interpretation of ground-truth data. From this output, aerial images were classified into detailed classes, the same procedure was hindered on the satellite images due to spatial resolution constraints. The sand class had the best overall accuracy (96%), due to its contrasts with surrounding objects. While the vegetation (i.e., pioneer saltmarshes) and algae classes had lower accuracy values (49.6–89.0%), possibly due to being still damp or covered in fine sediment This is a common challenge in transitional systems across land-water interfaces, such as wetlands, where the abiotic conditions (e.g. solar exposure, tides) fluctuate heterogeneously over time and space. The findings presented herein revealed the consider-

* Corresponding author.
*E-mail address:* fmafonso@fc.ul.pt (F. Afonso).

https://doi.org/10.1016/j.rsase.2024.101306
Received 27 September 2023; Received in revised form 2 July 2024; Accepted 16 July 2024
Available online 22 July 2024

able success of this approach. For the purpose of local decision-making, these are relevant outputs that can be replicated in other regions worldwide.

## 1. Introduction

Coastal and marine environments are highly valuable for society as a source of ecosystem services (Katsanevakis et al., 2011). Ecosystem-based marine spatial management can provide tools for the sustainable management of natural resources affecting the distribution of these services, while reducing the conflicts among stakeholders from different sectors (Katsanevakis et al., 2011). Natural capital assets (i.e., stock of natural resources (Constanza et al., 1997)) underpin each ecosystem service (i.e., the contribution of the environment to human well-being (Haines-Young and Potschin, 2013)), and collection of environmental data in detailed habitat maps allows the understanding of these assets (Hooper and Austen, 2020) while providing information to support decision-making in managing these resources (Lyons et al., 2018).

Remote sensing (RS) can be an effective and nondestructive method to acquire information about the Earth's surface (Liu, 2015; Randin et al., 2020). RS provides data at high temporal resolution and has the capacity to cover regions that are otherwise difficult to reach (Rocchini et al., 2017; Sogno et al., 2022). RS data availability has grown exponentially with enhanced satellite image sensor features, increased temporal and spatial resolution (Murray et al., 2018) and the use of airborne and UAV (Unmanned Aerial Vehicle) devices (Madden et al., 2015). Nevertheless, spectral satellite imagery is still dependent on weather conditions, (i.e., cloud coverage), UAVs surveys need appropriate launch-landing and georeferencing makers, which can be troubling in wetlands. Furthermore, UAV battery capacity is still short to cover large areas (Dronova et al., 2021), while airborne imagery is still expensive since requires specialised aircraft and qualified personnel (Abdelmajeed & Juszczak, 2024).

Satellite RS has been employed in intertidal habitat mapping, for instance, in seagrass meadows (Koedsin et al., 2016), kelp forests (Casal et al., 2011), saltmarshes (Li et al., 2010) and intertidal macroalgae (van der Wal et al., 2014). However, RS data use is still limited when capturing time-sensitive data (Wang and Yésou, 2018), and automatic data processing techniques require further developments, thus, there are still constraints to retrieving the information needed in a short period of time (Zhou et al., 2023). The tridimensionality of marine environments can also be a challenge for the use of RS data due to the biophysical properties of the water column (Kennedy et al., 2012; Roelfsema et al., 2013; Wulder et al., 2012). Products from the use of RS may not necessarily meet the desired levels of accuracy based on comparisons with reference data, which is typically assumed to be correct (Stehman, 2009). However, the use of RS datasets is mostly free, provides a large spatial and temporal coverage, and their applicability is continuously growing (Krause et al., 2023; Stratoulias et al., 2018). Together with powerful semi-automated classification algorithms, RS techniques can provide meaningful results in intertidal areas, representing an important cost-effective tool to study such systems at higher scales (Corbane et al., 2015; Hunter and Power, 2002; Piaser and Villa, 2023; Sun et al., 2021; Wang et al., 2019).

Estuarine wetlands shelter multiple ecological communities (Gray et al., 2018; Yu et al., 2023). The complex and dynamic estuarine environment, transitioning from terrestrial to aquatic types, still challenges the retrieval of detailed and fine-resolution maps using automatic classification algorithms due to the interaction of several factors, such as the limited size and rapid ecological dynamic of coastal habitats requiring detailed and frequent data collection (Valentini et al., 2015; Wang et al., 2024). In estuaries, expert knowledge is even more important to further understand the classification and is crucial to define class boundaries, especially when different vegetation possesses similar spectra (Valentini et al., 2015; Xie et al., 2008). Furthermore, most of the intertidal habitats are affected by tides. The variation on the water content can drastically impact the spectral signature of sediment and vegetation, an important feature that should not be overlooked (Rainey et al., 2003). The temporal mismatches of the ground data and the image acquisition should also be a factor when considering the method to capture RS data (Lugendo et al., 2024).

The application of the RS tools in the field of Ecosystem Service Assessment has great potential. These studies need reliant information on habitat and land use maps to identify potential ecosystem services (Barbosa et al., 2015). To understand the link between the ecosystem and human well-being is necessary to comprehend where to find these potential uses (Barbosa et al., 2015). Furthermore, changes in habitat or land use are the main drivers that influence ecosystem services provision, thus, mapping these changes can improve decision-making (Foley et al., 2005; MEA, 2005). However, even with all the developments in RS technology and methodologies, the contribution for Ecosystem Service Assessments has been insufficient (Andrew et al., 2014; Feld et al., 2010; Tallis et al., 2012). Thus, the novelty of this study lies on the combination of complementary data sources, with different features (i.e., spatial resolution, band information, etc.) to overcome existing challenges associated with the fact that estuaries are composed of intertidal (strong influence of water) areas that are heterogenous, patchy and fragmented at different scales. Hence, the main goal of this study was to integrate different approaches to perform habitat mapping in the scope of an Ecosystem Service Assessment, by using semi-supervised image classification, using two RS products with different spatial resolutions: i) satellite images from Planet Scope (3 m resolution); and ii) aerial photography (20 cm resolution). This approach was used to map the intertidal habitats of the Sado Estuary to identify and quantify the units that provide ecosystem services to the local community.

## 2. Methodology

### 2.1. Study area

The Sado estuary (Fig. 1) has an area of approximately 180 $km^2$ and belongs to one of the largest Portuguese hydrographic basins, Sado river basin (7692 $km^2$ – Feio and Ferreira, 2019). The water column of the Sado estuary is well-mixed due to a strong tidal influence, the main force of water circulation, associated with the short water column and exposure to winds (Biguino et al., 2021; Santos

et al., 2022). Sado is a mesotidal estuary with semidiurnal tides which can rise to 3.9 m at high water (Brito, 2009; Ferreira et al., 2005). Tidal mixing in the Sado occurs through the mouth of the estuary, which is ~2 km wide (Castro, 1997; ICNF, 2008). Nowadays, the Sado Estuary is a Natural Reserve and is protected by several international conventions (i.e., Natura, 2000; RAMSAR - ICNF, 2008).

The estuarine intertidal area is dominated by mudflats and sandbanks, and the adjacent land is mostly used for agriculture (i.e., pasture, rice crops, cork plantation – Fig. 1, ICNF, 2008). The area is divided into two main regions: the central bay (Setúbal bay and Marateca channel) and the Alcácer channel (Coutinho, 2003). The central bay has always been an essential industrial trade centre due to the presence of the Setúbal port located at a major intercontinental navigation route (Nunes et al., 2019). Tróia Peninsula, located in the Setúbal bay, is prominently situated in the south margin of the estuary and is dominated by tourist resorts (Fig. 1, Coutinho, 2003). The Marateca Channel is characterized by the presence of aquaculture ponds and abandoned salt pans, however, nowadays many are converted into shellfish and fish farms, which are also important nesting sites for birds (Fig. 1, ICNF, 2008). Due to the many different uses of the area, the estuary has been highly modified and urbanized to accommodate all the activities. For example, over the years, the main channel has been dredged as a means to maintain the navigability of the estuary (Conceição, 2016; van Maren et al., 2015).

### 2.2. Datasets

Habitat mapping was performed using two different sources of information to provide a seamless evaluation of the habitats at high resolution. Very-high resolution satellite images and orthophotographs were used for the classification of the habitats, as described below. This allowed assessment of habitat features at two different resolutions, i.e., comprehension of different Sado areas at different spatial scales and improvement of the final accuracy.

#### 2.2.1. Satellite data

Planet Scope level 3b imagery for the relevant area was acquired through Planet Labs' Data API. It has a spatial resolution of 3 m and 8 colour bands (Table 1; Planet Team, 2017). Two aspects were considered for the selection of satellite images: i) minimum cloud percentage (0%) and ii) lowest tide at the time of acquisition. The product obtained was captured on May 1st of 2022 by the SuperDoves (PSD.SD) sensor. The PSD.SD provides a framed scene within a strip, a continuous narrow band of earth scanned by the sensor, each strip contains several overlapping scenes. The scenes collected to cover the study area had a total area of 637 km$^2$. The data were provided in a GeoTiff format projected into the UTM (Universal Transverse Mercator) projection using the WGS84 Datum, orthorectified to avoid terrain distortions, and radiometrically calibrated. The products were delivered corrected from atmospheric effects, which consists of converting and correcting the top of atmosphere reflectance to bottom-of-atmosphere reflectance, this is an important step to avoid errors and inaccuracies (PlanetLabs).

#### 2.2.2. Orthophotograph data preparation

In the scope of the project *ORTOSado-2021*, the orthophotographs were collected on the 7th and October 8, 2021 with a total covered area of 355 km$^2$ (Melo and Nogueira Mendes, 2022a). The images were converted into the projected coordinate system ETRS89-PTTMO6 and collected with a resolution of twelve bit, then orthorectified using OrthoMaster with a spatial resolution of 20 cm and

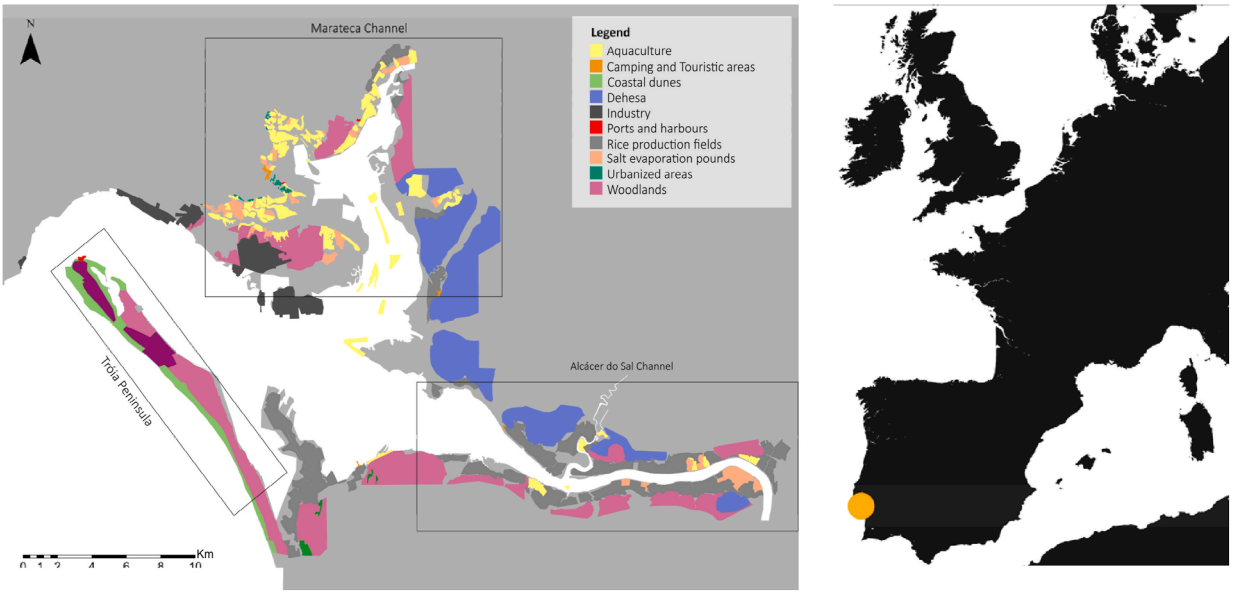


**Fig. 1.** Sado estuary map (left inset) and location context of the study area in Iberian Peninsula (orange dot in right inset). (For interpretation of the references to colour in this figure legend, the reader is referred to the Web version of this article.)

**Table 1**
Original wavelength of Sensor PDB.SD colour bands.

| Band name | Wavelength (fwhm) | | |
|---|---|---|---|
| | Min | Max | Average |
| Coastal Blue | 431 | 452 | 443 |
| Blue | 465 | 515 | 490 |
| Green I | 513 | 549 | 531 |
| Green | 547 | 583 | 565 |
| Red | 600 | 620 | 610 |
| Yellow | 650 | 680 | 665 |
| Red Edge | 697 | 713 | 705 |
| Near-InfraRed (NIR) | 845 | 885 | 865 |

four bands (RGB and NIR). The OrthoVista software was used to analyze and correct the images, the sun reflection and chromatic differences between the different maps were removed (Melo and Nogueira Mendes, 2022a).

### 2.3. Selection of habitats for this study

The available datasets for this study have different levels of spatial resolution, thus, different degrees of habitat specificity depending on image resolution were defined. EUNIS (European Nature Information System; https://eunis.eea.europa.eu/) is particularly useful in this case since it provides a comprehensive hierarchical description of habitats occurring throughout Europe. For the satellite images four cluster classes were considered, while the orthophotographs were classified into six classes (Table 2). Cluster classes are groups formed by the aggregation of the classes and are easier to detect in products with coarser image resolution.

Sometimes it was not possible to apply visual interpretation due to confusion between classes, the Normal Difference Vegetation Index (NDVI) was used instead to efficiently distinct vegetation classes. This index is used to enhance the vegetation features, to defined thresholds, thus it can be a valuable tool to better differentiate mud from microphytobenthos (MPB), and MPB from filamentous algae (Table 2; Bertels et al., 2011; Brito et al., 2013; Haro et al., 2022)). A cluster class called intertidal water was also defined to comprehend the differences in tidal levels between satellite image and ortophotographs (Table 2). This cluster class in the satellite image was mainly represented by open water, however, in the lowest tide of the orthophotographs a mixture of classes was present. Furthermore, gravel and sand could not be separated in the images due to gravel being poorly represented across the estuary (Traganos et al., 2022). Mud covered with microphytobenthos was considered to be a class in its own right due to its ecological importance, despite being an algae community instead of a habitat.

### 2.4. Image pre-processing – masking land and water

Image pre-processing and processing tasks were performed in ArcGIS Pro v3.0.1. First, all the orthophotographs were mosaicked to obtain only one raster file. The process was replicated for the satellite image stripes to create one mosaic of the area containing both types of data.

In the pre-processing step (Step 1 in Fig. 2), masks were created using orthophotographs that enhance each class's features (Traganos and Reinartz, 2018). The water mask resulted from the Normalized Difference Water Index (NDWI), which allows the detection of water bodies, applied to the orthophotographs since these were captured in the lowest tide possible (−1.7 m referred to Mean Sea Level). The index is based on the Green and Near-infrared (NIR) bands following the expression (Green − NIR)/(Green + NIR), assuming that there is a decrease in the reflectance of water in the NIR compared to the visible spectrum (Ghuffar, 2018; McFeeters, 1996). Although using the Modified Normalized Difference Water Index, which uses Shortwave-infrared (SWIR) instead of NIR, might provide better results in water masking (Xu, 2006), the absence of the SWIR band in the orthoimagery product inhibits the use of this index. The land mask for the orthophotographs was produced by experts (with local knowledge) based on manual photointerpretation. The seagrasses mask (Melo and Nogueira Mendes, 2022b) was also developed by local experts on seagrass

**Table 2**
Classes identified for satellite image (cluster classes) and orthophotographs (classes) classification, and the identification tools used to map each class.

| Cluster Classes | Classes | Identification Tools |
|---|---|---|
| Sand | Sand | Ground truth; Manual photointerpretation |
| Mud | Mud | Ground truth; NDVI $<0.0$ |
| | Microphytobenthos | Ground truth; $0.01<$ NDVI $\leq 0.3$ |
| | Filamentous algae | Ground truth; NDVI $>0.3$ |
| Saltmarshes | Pioneer saltmarshes<br>Saltmarshes (low to high) | Ground truth; Manual photointerpretation |
| Intertidal Water | Sand | Ground truth; Manual photointerpretation |
| | Mud | Ground truth; NDVI $<0.0$ |
| | Microphytobenthos | Ground truth; $0.01<$ NDVI $<0.3$ |
| | Filamentous Algae | Ground truth; NDVI $>0.31$ |

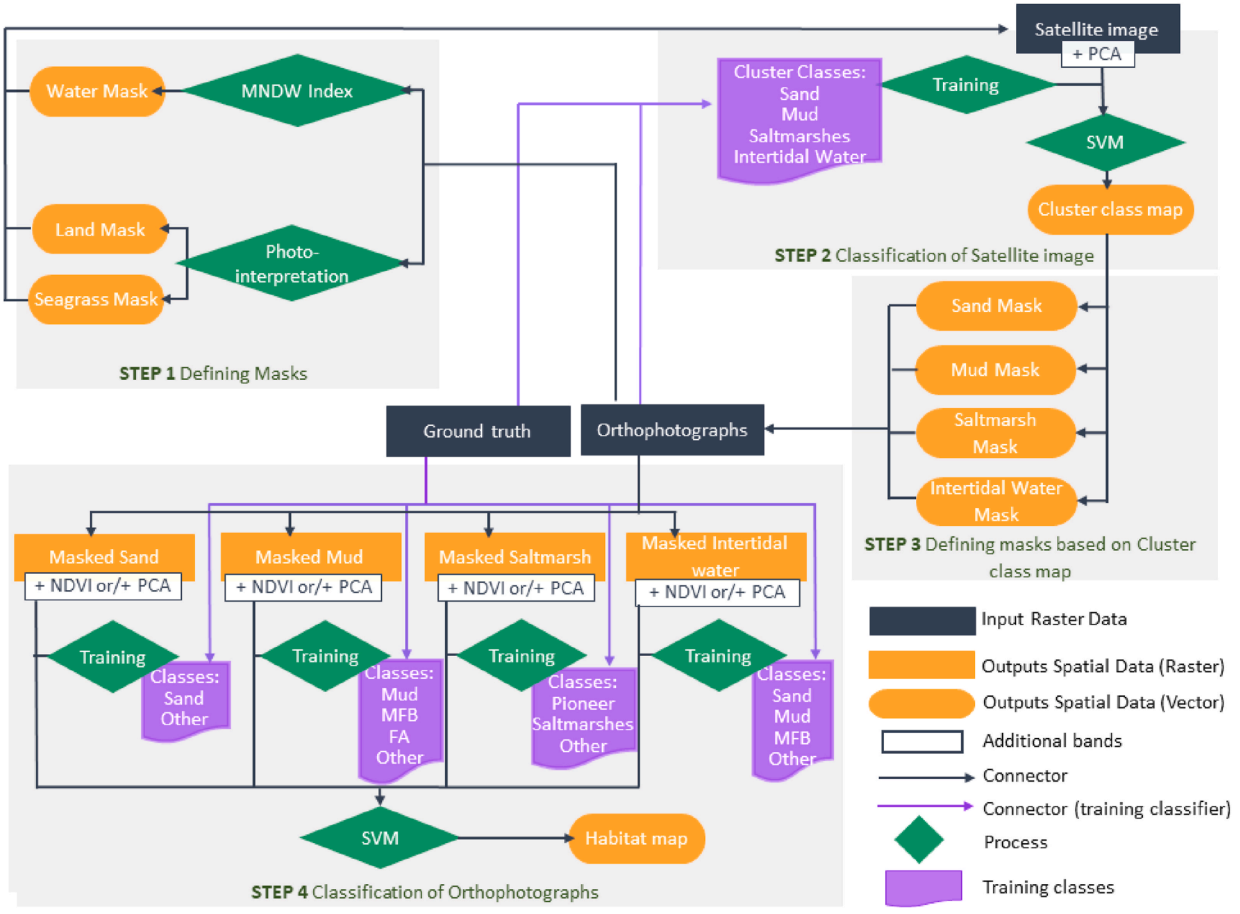


**Fig. 2.** WorkFlow describing the process of building masks throughout the classification. In the ortophotograph classification, when training the classifier, besides the classes listed before, an "Other" class was also considered to clearly identify classes that did not belong to the target classes. FA - Filamentous Algae; MPB - Microphyto-benthos; SVM - Support Vector Machine.

identification who identified this class through photointerpretation of the orthophotographs together with ground truth data digitized in a GIS environment, and polygons from ORTOSado-2021 (Melo and Nogueira Mendes, 2022a).

### 2.5. Image processing

After masking the RS imagery, the satellite image was classified, subsequently, the orthophotographs were classified.

#### 2.5.1. Adding extra bands to satellite images

In Step 2 (Fig. 2), to reduce the variance of the satellite image features, an extra band was added to the product's original 8 colour bands (Table 1), which was combined using Principal Component analysis (PCA, **Supplement Material S1**), similar to other RS studies (Chen et al., 2022). PCA has been widely used in RS in different contexts, including classification procedures (Gómez-Palacios et al., 2017; Rodarmel and Shan, 2002). It adapts the correlation among the original bands by reducing high dimensional vectors to maximizes the covariance and reduce the redundancy, highlighting the important information (Gómez-Palacios et al., 2017; Koonsanit et al., 2012; Rodarmel and Shan, 2002).

#### 2.5.2. Satellite image classification

The composite of 8 bands/PCA band was classified using a supervised pixel-based analysis (i.e., categorical judgements based on the spectral signature of each individual pixel (Gong and Howarth, 1990)), using the classifier Support Vector Machine (SVM), resulting in a map categorized in 4 cluster classes (Table 2; Step 2, Fig. 2). SVM is considered one of the most efficient pixel-based classifiers for land-cover classifications (Boyd et al., 2006; Dalponte et al., 2009; Dixon and Candade, 2008; Keramitsoglou et al., 2006; Pal and Mather, 2005). SVM is a non-parametric supervised learning classifier (Zhang, 2015), based on the statistical learning theory of Vapnik (1995). The classifier uses support vectors to train samples located near the decision boundary between classes to classify the input dataset into a predefined number of classes, and does not rely on the data distribution (Boyd et al., 2006; Oommen et al., 2008).

#### 2.5.3. Training the classifier

To train the SVM algorithm, training classes were defined based on manual photointerpretation of orthophotographs and ground truth data. Campaigns of ground truthing for validation purposes occurred from October 2021 until August 2022, and used 572 pictures taken with a digital camera to train the algorithm, comprising 75% of the total captured pictures (Lyons et al., 2018, Table 2). All pictures taken were geo-referenced, and an effort was made to try to capture transition zones and identify differences in photosynthetic material found in the sediment, such as MPB and filamentous algae. Identifying these habitats was difficult because sediments, especially mud, contaminate the biological signal acquired from sediments. For instance, to distinguish the 2 classes of saltmarshes, pioneer saltmarshes and low to high saltmarshes, identification of the species *Spartina maritima* was used as this species is usually only present in pioneer saltmarshes (EUNIS, 2012), and is easy to identify from its morphology, sparse distribution and darkened colour.

In Step 3 (Fig. 2), each cluster class was used as a mask to clip over the orthophotographs in smaller areas.

#### 2.5.4. Adding an extra band to the clipped orthophotographs

Step 4 (Fig. 2) consisted of the classification of orthophotographs after being masked out (i.e., sand, intertidal water, saltmarsh, mud). Once again, as for the satellite images, extra bands were added to the VNIR bands of the orthoimagery. In this case, the extra bands were PCA band combination and the NDVI. Different classification schemes were tested, and depending on the best accuracy detected each class had a different extra band (Table 3 based on Supplementary material S1).

#### 2.5.5. Orthophotographs classification

The composites from section 2.5.4**.** were classified using the SVM (sections 2.5.2**.** and **2.5.3.**). After the classification process and estimation of all classes, final maps were produced for each dataset used. The colouring of the maps was selected based on the proximity to the actual class colour, and the differentiation between all (i.e., lighter and darker colours), to make it more accessible to colour-blind people.

### 2.6. Accuracy assessment

The accuracy value is a report describing the agreement between mapped values and ground data (Lyons et al., 2018). Accuracy was assessed through ground truthing campaigns (see Section 2.5.1). A total of 177 captured pictures were used to provide reference points, 500 points distributed equally within all the classes. The output, an error matrix, can be used to calculate the producer, users, and overall accuracy. The producer's accuracy is a measure of the probability that the reference samples are correctly labelled and the user's accuracy is an indicator of the probability that a classified pixel accurately represents the ground truth data (Gxokwe et al., 2022). While both are informative, the overall accuracy is more meaningful because it measures the efficiency of the algorithm by estimating the mean of the producer and user's accuracy. Thus, in this study, overall accuracy was selected as the preferred method. The accuracy is used as an estimate of error or uncertainty of the output classification, enabling choice of the most appropriate mapping procedure or informing the interpretation of the output (Lyons et al., 2018). Thus, based on the overall accuracy of the different classification schemas (extra bands to used) it was decided which extra bands would be used to estimate the final map (Supplementary material S1).

## 3. Results

### 3.1. Image classification maps

Based on the EUNIS classification system (EUNIS, 2012), a satellite image was classified into four cluster classes (Fig. 3), and presented a higher classified area of mud, largely found in all the study area (Table 4).

To improve accuracy and detail around the muddy habitats, a second map with higher spatial resolution was created, consisting of six cluster classes, with microphytobenthos covered mud being the most dominant class.

### 3.2. Accuracy assessment

The accuracy of orthophotograph classification (Fig. 4) was based on ground truth data. The sand class (Sand cluster class) presented the higher values in all the accuracy calculated (>95%, Table 5). All the classes presented an overall accuracy higher than

**Table 3**
Extra bands added to each masked raster (besides VNIR bands). Grey cells indicate no use of extra bands. Saltmarshes class includes all habitats from low to high saltmarshes.

| Cluster class | Class | Extra band |
|---|---|---|
| Sand | Sand | PCA |
| Mud | Mud | - |
| | Microphytobenthos | - |
| | Filamentous algae | NDVI + PCA |
| Saltmarshes | Pioneer saltmarshes | NDVI |
| | Saltmarshes | NDVI + PCA |
| Intertidal water | Sand | NDVI |
| | Mud | - |
| | Microphytobenthos | - |
| | Filamentous algae | - |

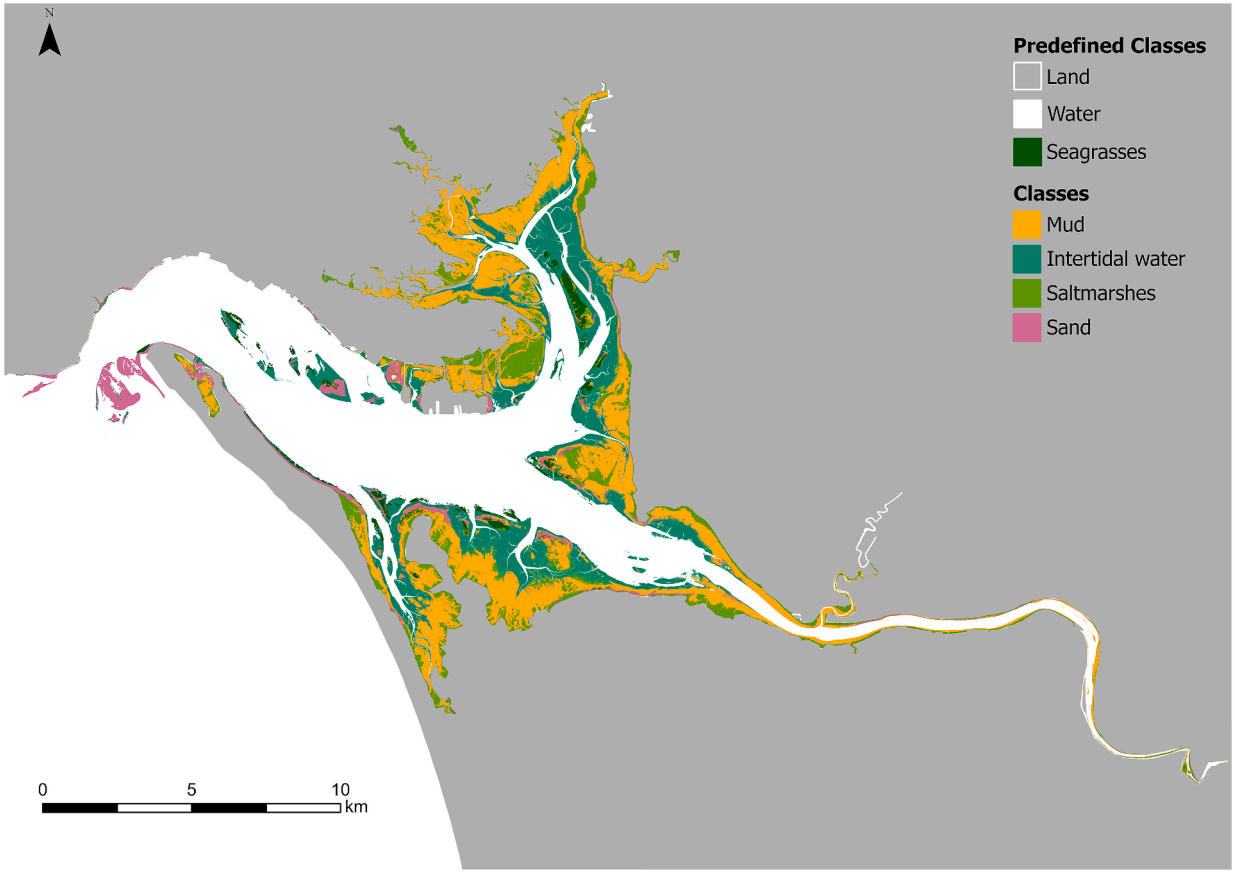


**Fig. 3.** Habitat map including the cluster classes and the predefined classes (masks).

**Table 4**
Total classified areas ($km^2$) of each cluster class and class. Saltmarshes class includes all habitats from low to high saltmarshes.

| Cluster classes | | Classes | |
|---|---|---|---|
| Sand | 5.22 | Sand | 3.31 |
| Mud | 35.82 | Mud | 11.97 |
| | | Microphytobenthos | 19.19 |
| | | Filamentous algae | 1.77 |
| Saltmarshes | 13.78 | Pioneer saltmarshes | 1.73 |
| | | Saltmarshes | 6.45 |
| Intertidal water | 23.65 | Sand | 9.65 |
| | | Mud | 2.80 |
| | | Microphytobenthos | 6.29 |
| | | Filamentous algae | 1.55 |

50%, except for the filamentous algae (Mud cluster class, Table 5). The user's accuracy was higher for the mud and filamentous algae class (Intertidal Water cluster class), with minimal values in the microphytobenthos class (Mud cluster class, Table 5). The producer's accuracy was higher in the saltmarshes (Saltmarshes cluster class) while presenting a low value for filamentous algae (Mud cluster class, Table 5).

## 4. Discussion

A supervised pixel-based classification algorithm on remote sensing images enabled the intertidal area of the case study Sado estuary to be mapped. Two output maps were created using data with distinct spectral, temporal, and spatial resolutions. The two different spatial scales allowed the assessment of the ecosystem from distinct approaches. In this way, it was possible to achieve high accuracy, which can be challenging, especially in wetlands (Ozesmi and Bauer, 2002) due to the dynamic and complex nature of existing habitats and communities in wetlands.

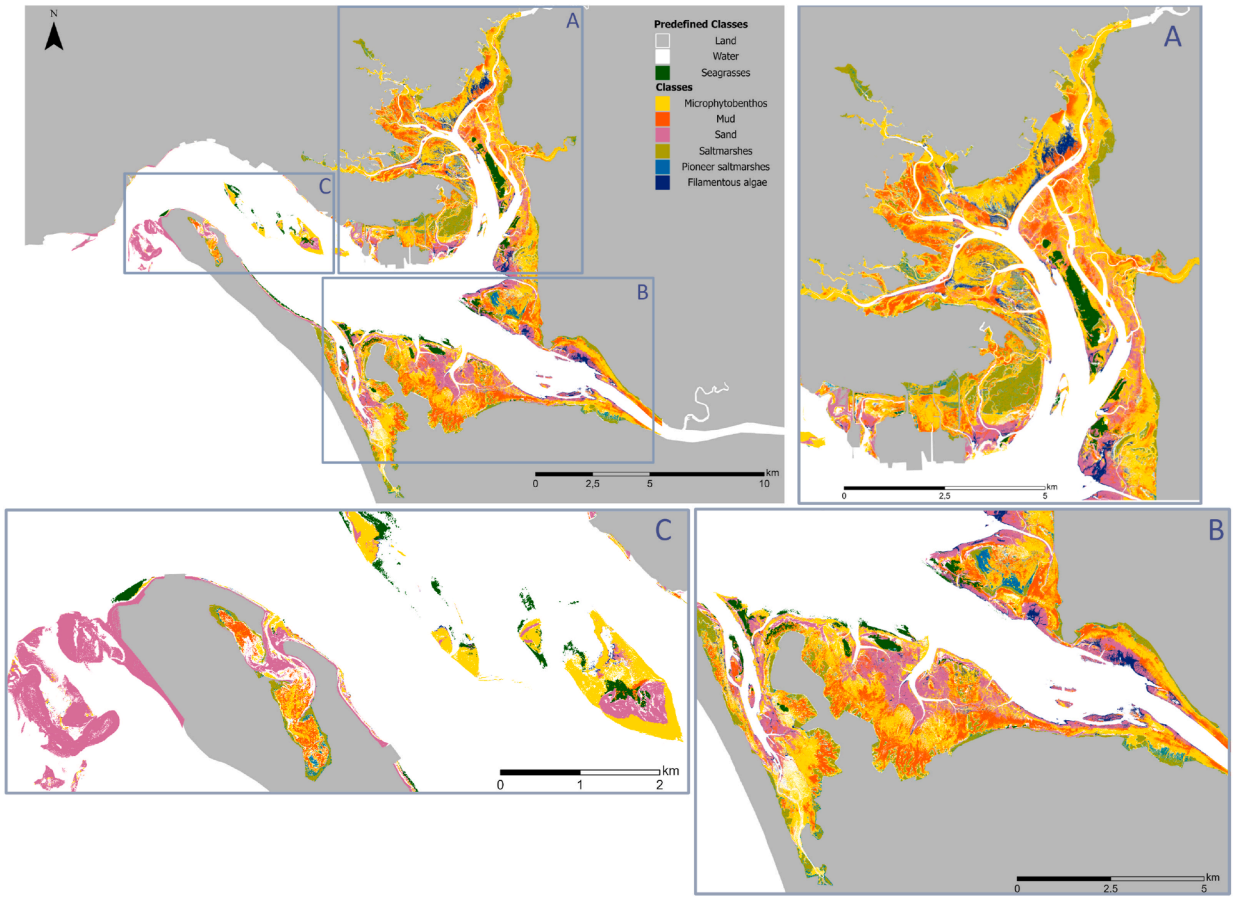


**Fig. 4.** Classification of Orthophotographs (right top inset) and inset zooms of 3 zones of the study area. Saltmarshes class includes all habitats from low to high saltmarshes.

**Table 5**
Classification accuracy values for the user (U), producer (P) and overall (O). Saltmarshes class includes all habitats from low to high saltmarshes.

| Cluster Class | Class | U | P | O |
|---|---|---|---|---|
| Sand | Sand | 95.8 | 96.2 | 96.0 |
| Mud | Mud | 81.3 | 83.9 | 82.6 |
| | Microphytobenthos | 59.5 | 70.9 | 65.2 |
| | Filamentous algae | 80.0 | 19.2 | 49.6 |
| Saltmarshes | Pioneer saltmarshes | 72.9 | 59.9 | 66.4 |
| | Saltmarshes | 72.5 | 96.9 | 84.7 |
| Intertidal Water | Sand | 69.7 | 88.3 | 79.0 |
| | Mud | 95.3 | 83.5 | 89.4 |
| | Microphytobenthos | 80.8 | 63.0 | 71.9 |
| | Filamentous algae | 96.4 | 81.6 | 89.0 |

### *4.1. Challenges of habitat mapping*

Coastal wetlands are known for their habitat diversity and complex organization. Thus, mapping these habitats represents an important challenge, especially when different habitats share similar spectral signatures such as mud covered with filamentous algae and seagrass (Jiao et al., 2019). In general terms, the dominant method usually applied in these systems is the classification based on pixel, particularly in cases where objects are smaller than the pixel (Blaschke et al., 2014; Calleja et al., 2019; Ozesmi and Bauer, 2002). However, several limitations have been identified in the literature, such as the *salt and pepper* pixel effects that occur when using pixel-based analysis in high-spatial resolution imagery, which are caused by the interference of neighboring pixels with different habitats (Ouyang et al., 2011). Furthermore, the fact that most of the classes can happen in very small areas, at a sub-pixel level, may lead to under or over-estimation of those classes (Traganos et al., 2022).

Several studies have found that the SVM algorithm can outperform other classifiers with higher accuracy (Dixon and Candade, 2008; Li et al., 2012; Qing et al., 2010; Zhong et al., 2007). It is especially suited for cases with limited amount of reference data

(Mountrakis et al., 2011) and classification of multiple classes (Knerr et al., 1990), thus, it is appropriate for estuarine systems. The high success rate of SVM has been justified with the fact that it does not assume normality in data distribution, thus, the classifier based on the training data can make assumptions to categorize the areas where no data is available (Mountrakis et al., 2011). However, the algorithm is not able to deal with data collected with limited precision or atmospheric distortions (Mountrakis et al., 2011). One of the emerging issues in the use of supervised classifiers is the lack of standardized amount of training and validation data to match the imagery resolution and extension (Traganos et al., 2022). The oversampling can lead to a biased classification (Aplin, 2006; Cushnie, 1987; Hsieh et al., 2001; Timm and McGarigal, 2012).

Usually, higher accuracy is reached when simple categories are identified, for instance the sand has a spectral signature completely different from the rest of the habitats. Hence, signature contamination is less common. Tides can have a significant impact on the classification of muddier sediment, bare mud is easily confused with vegetated habitats with less density (e.g., microalgae communities, seagrasses). Tidal influence can change the spectral signature of habitats due to the water content (Pe'eri et al., 2016). Considering the dynamics of an estuarine system, the long tidal delays can be a limitation when trying to map intertidal habitats, for instance, Sado tidal delay can go up to 1h10 at the most upstream point (Alcácer do Sal, Andrade et al., 2006). To discriminate between bare mud and microalgae-covered mud, a decrease in reflectance in the NIR (Near-Infrared wave) indicates residual absorption by chlorophyll-*a* or phaeopigments present in the algae (Kromkamp et al., 2006). These communities, microphytobenthos (MPB), are a major contributor to the total organic production in coastal areas (Asmus and Asmus, 2000; Frankenbach et al., 2020; Haro et al., 2020; Underwood and Kromkamp, 1999). However, the detection of MPB goes beyond the identification of chlorophyll-*a* in the sediment, the signature spectrum of MPB is a complex relation between several variables (i.e., pigment composition, sediment type, water content). For instance, Oiry and Barillé (2021) wrongly classified MPB as mud, while bare mud and sand were correctly classified as such. One possible solution to better identify these communities is by setting empirical NDVI thresholds. The vegetation reflects strongly in the NIR and absorbs radiation in the red band, the NDVI index uses the ratio between both wavelengths to distinguish vegetated and non-vegetated areas without overestimating these communities (Jensen, 2006; Mather, 1999). Moreover, this vegetation index can be applied in a wide range of situations due to its low sensitivity to sediment background influences (Barillé et al., 2011). However, this is not a straightforward method. It is influenced by several variables, namely water content and thin sediment covering the algae, which increases the chance that light can interact with more than one component of the substratum (Tian et al., 2010). Other studies have also shown that commonly used vegetation and water indices have not been very effective in discriminating vegetation species in wetland environments (Gupta et al., 2018; Zhang et al., 2011).

Saltmarshes occupy large areas distinctly different from neighboring intertidal habitats, these are relatively stable habitats throughout the year since most of the vegetation is persistent, even though with poorly defined boundaries (Thomson et al., 2003; Tiner, 2015). However, pioneer saltmarshes are more difficult to distinguish from some other habitats in the mosaic. Located in the lowest intertidal zone and dominated by the *Spartina* genus, they usually present vegetation that is much shorter and darker, similar to habitats dominated by mud or algae communities (Sousa, 2006). Pioneer saltmarshes spectral signature is easily confused with other habitats which explains the lower accuracy values detected (66.4%). Other studies presented lower accuracy for saltmarshes than in this study (64.7 % vs 84.7%, respectively - Alam and Hossain (2021)).

To understand and improve the outcomes the uncertainty associated with them must be known, and that knowledge must be incorporated in the decision process (Burgman et al., 2005; Foody, 2015).The aim of the accuracy assessment is to assess the error associated with the classification which can be used to correctly interpret the outputs (Lyons et al., 2018). There are several metrics that can be used, however, none of them have been fully accepted as the standard method (Lyons et al., 2018) and many studies fail to achieve the target accuracy (OA > 85% - Foody, 2010). For example, the Kappa accuracy (predicts the difference between actual agreement and random agreement (Congalton, 1991)) has been criticized by the comparison with randomly selected pixels (Lyons et al., 2018). On the other hand, the Overall accuracy has been criticized because there is no assurance that classes are accurately classified due to the algorithm efficiency or whether accurate classification happens by chance (Foody, 2002). The use of more than one metric to optimize the classification has been suggested (Morisette and Khorram, 2000), even though the use of more than one method can cause conflict in the interpretation of the data (Stehman, 1997). Despite these issues, the comparison of some of the measures can help in the identification of problems in the classification process. For instance, if the producer's accuracy is much lower than the user's accuracy, this means that the area classified matches the reference data, however, the classifier failed to capture a fair amount of this class causing the under-estimation of some classes (Traganos et al., 2022). This is particularly significant in the filamentous algae class (Mud cluster class) where the user's accuracy is 4 times the producers, also this is the class with the smaller extension in the final map (total area of 3.32 $km^2$).

Additionally, some constraints may arise when collecting ground data. For instance, in estuarine systems, such as the Sado case study, physical access to the intertidal areas is limited due to property rights of landowners at the margins (e.g. farmhouses, aquaculture tanks) and also terrain constraints, this can affect the quality of the data collected (Edwards et al., 1998; Estes et al., 1999). To get significant accuracy assessment the collection of ground data must cover all habitats evenly (Foody, 2002), even small errors in the reference data set can cause a large bias in the accuracy measures, making it difficult to make simple generalizations of their effect (Alonzo et al., 2002; Hawkins et al., 2001; Vacek, 1985; Valenstein, 1990).

### *4.2. Combining satellite and orthophotographs: difficulties and challenges*

During the 2-step classification, the satellite images were mapped in cluster classes, while the orthophotographs were mapped in classes. In theory, the cluster classes would represent the sum of all classes within them. However, when comparing both classification outputs it is evident that there is an overestimation of the area of the cluster classes. This was expected since the broader spatial resolution has less sensitivity to the features of each cluster class, this can cause overestimation of the areas mapped. Namely the ex-

tent of the Sand cluster class was 5.22 $km^2$, while the same class only occupied an area of 3.31 $km^2$. Another factor that increases the discrepancy between the areas obtained from the different classifications is the coverage of each image, for instance the Planet Scope area includes all the estuary from its mouth up to Alcácer do Sal city, whereas the orthophotographs covers a much smaller area, which does not include the Alcácer do Sal channel (Fig. 1). The Saltmarshes cluster class had a total area of 13.78 $km^2$, however, the total area of the corresponding classes in the orthophotographs (saltmarshes and pioneer saltmarshes) was only 8.18 $km^2$. This discrepancy cannot be explained by considering the area not included in the orthophotos as saltmarshes in the Alcácer do Sal channel only occupy an area of 1.09 $km^2$. Thus, a significant area is not accounted as saltmarshes (4.5 $km^2$). The same issue was identified in the Sand and Mud cluster class, however, the area not accounted for is much smaller (1.7 $km^2$ and 1.29 $km^2$, respectively). Possibly, the sand closer to the water body can have some water content, presenting as darker than usual and with a spectral signature similar to mud causing the occasional confusion with the 2 classes. This is a spatially specific problem since the pictures were captured during the low tide, and the dry sand has a spectral signature completely distinct from any of the other classes considered. It has previously been noted that specific features of the Planet imagery can limit their application (Cooley et al., 2017; Houborg and McCabe, 2016; Poursanidis et al., 2019; Traganos et al., 2020). For instance, high levels of noise and low radiometric quality, as well as a low correlation between VIR and NIR bands, decreases the image quality and limits the use of them (Cooley et al., 2017; Poursanidis et al., 2019; Traganos et al., 2020; Wicaksono and Lazuardi, 2018). The combination of these features lowers the advantage of having higher spectral resolution in the satellite images, resulting in the overestimation of certain habitat areas.

### *4.3. Added values of combining different data sources and overall applications*

RS and semi-automatic classifiers are useful tools to map ecosystems, and to evaluate the extent and fragmentation of habitats (Bateman et al., 2011; Mace et al., 2015). This is an important step within an ecosystem service assessment since it enables identification of the units (i.e., habitats) providing services and benefits to the local communities (O'Higgins et al., 2010).

Furthermore, techniques for habitat mapping are required by local and national authorities responsible for ecosystem monitoring, for whom methods that involve less financial and time investment are especially useful (Samiappan et al., 2017; Weires et al., 2004). For research studies frequently undertaken in situations where there is both limited funding and time to undertake field surveys the use of different and free data sources (i.e., Planet Labs *Educational and Research Program*), in combination with the use of software licensed by universities (i.e., ArcGIS Pro) can help to overcome such challenges (Iglseder et al., 2023). However, acquiring accurate and detailed maps requires proper data which can be expensive and arduous (Najjar et al., 2017). The advances in space technology have led to an increase in resolution and affordability of satellite images (Dash and Ogutu, 2016). Nevertheless, the exclusive use of satellite images was not able to identify the habitats encompassed by the study area with sufficient resolution. This was only achieved when satellite images were complemented with the use of aerial photographs. Thus, the aim of the mapping process must be considered before determining the details needed and any possible future requirement to enhance the accuracy of the outputs. For instance, this study was developed in the context of ecosystem management. Thus, the goal was not to get the best accuracy possible, but to be able to use simple and efficient methods supported by expert knowledge to rapidly produce outputs that would be sufficiently detailed and accurate for the purpose of ecosystem service assessment.

Over the last few years, great progress has been made in the study of coastal habitat mapping, some suggestions to improve the accuracy of classification include hybridization of different machine-learning classification algorithms and the use of object-based classification algorithms (Aroma and Raimond, 2016). Moreover, it has been suggested the integration of LiDAR sensors in UAVs to effectively map small habitats with high-resolution and exceptional detail (Banerjee and Raval, 2022). However, such approaches still require a large amount of data that are only available for specific areas, hindering its application in low-income countries. In the future, it would be interesting to put in practice some of these suggestions to enhance the accuracy or detail of the maps. With the development of new cutting-edge technologies over the next years, the implementation of hyperspectral sensors in earth observation programs (e.g. Landsat Next - https://landsat.gsfc.nasa.gov/satellites/landsat-next/) and the dissemination of datasets acquired in the framework of many projects, data can become more accessible and tailored to improve habitat mapping accuracy and detail.

## 5. Conclusions

Coastal ecosystems are under increasing pressure, thus it is crucial to invest in methods to better understand and increase the knowledge about these systems (Murray, 2018). The use of remote sensing and semi-automatic classifiers is viewed as a win-win solution in the literature (Islam et al., 2008; Saul and Purkis, 2015), given their potential to enable the production of detailed habitat maps with little (time and financial) investment compared to field observations. In this study, satellite images and orthophotographs were used to create a habitat map for ecosystem service assessment. The overall accuracy for each habitat class ranged from 49.6 to 96%, with less accurate results for habitats with lower vegetation (i.e., pioneer saltmarshes) and higher accuracy for habitat classes with spectral signatures that were very different from other habitats.

## Ethical statement

The authors declare that they followed all ethical practices in relation to the development, writing and publication of the article.

## Funding

F. Afonso received a PhD grant (2020.06997.BD) from Fundação para a Ciência e a Tecnologia (FCT). Furthermore, F. Afonso and S. Broszeit were supported through PORTWIMS, funded by the European Union's Horizon 2020 Research and Innovation Programme

(810139). A.C. Brito was also partly funded by FCT through the Scientific Employment Stimulus Programme (CEECIND/00095/2017). FCT also supported C. P. Lira through an employment contract (DL57/2016/CP1479/CT0079, https://doi.org/10.54499/DL57/2016/CP1479/CT0079). This work benefited from the Infrastructure CoastNet (http://geoportal.coastnet.pt), funded by FCT and the European Regional Development Fund (FEDER), through LISBOA2020 and ALENTEJO2020 regional operational programmes, in the framework of the National Roadmap of Research Infrastructures of strategic relevance (PINFRA/22128/2016). This study had the support of FCT through the strategic project UIDB/04292/2020 awarded to MARE (https://doi.org/10.54499/UIDP/04292/2020) and through project LA/P/0069/2020 granted to the Associate Laboratory ARNET (https://doi.org/10.54499/LA/P/0069/2020).

## CRediT authorship contribution statement

**F. Afonso:** Conceptualization, Formal analysis, Investigation, Methodology, Software, Validation, Visualization, Writing – original draft. **C. Ponte Lira:** Conceptualization, Methodology, Supervision, Writing – review & editing, Validation. **M.C. Austen:** Supervision, Writing – review & editing. **S. Broszeit:** Supervision, Writing – review & editing. **R. Melo:** Resources, Writing – review & editing. **R. Nogueira Mendes:** Resources, Writing – review & editing. **R. Salgado:** Resources, Writing – review & editing. **A.C. Brito:** Conceptualization, Supervision, Validation, Writing – review & editing.

## Declaration of competing interest

The authors declare the following financial interests/personal relationships which may be considered as potential competing interests:

F. Afonso reports financial support was provided by Fundação para a Ciência e Tecnologia. F. Afonso reports financial support was provided by EU Horizon 2020 Research and Innovation Programme. S. Broszeit reports financial support was provided by EU Horizon 2020 Research and Innovation Programme. A. C. Brito reports financial support was provided by Fundação para a Ciência e Tecnologia.

## Data availability

No data was used for the research described in the article.

## Acknowledgements

All the authors want to acknowledge the importance of the Planet Labs *Educational and Research Program* for allowing the compilation of images with high spatial and spectral resolution without any costs. Also, a special thanks to ICNF member, Ana Sofia Palma, for all their help in acquiring GIS information about the study area. Moreover, the authors are very thankful to Adriana Carvalho and Mariana Marques for their participation in the fieldwork.

## Appendix A. Supplementary data

Supplementary data to this article can be found online at https://doi.org/10.1016/j.rsase.2024.101306.

## References

Abdelmajeed, A., Juszczak, R., 2024c. Challenges and limitations of remote sensing applications in northern peatlands: present and future prospects. constanz. Rem. Sens. 16 (3), 591. https://doi.org/10.3390/rs16030591.

Alam, S.M.R., Hossain, M.S., 2021. A rule-based classification method for mapping saltmarsh land-cover in south-eastern Bangladesh from Landsat-8 OLI. Can. J. Rem. Sens. 47, 356–380. https://doi.org/10.1080/07038992.2020.1789852.

Alonzo, T.A., Pepe, M.S., Moskowitz, C.S., 2002. Sample size calculations for comparative studies of medical tests for detecting the presence of disease. Stat. Med. 21, 835–852. https://doi.org/10.1002/sim.1058.

Andrade, C., Freitas, M.C., Brito, P., Amorim, A., Barata, A., Cabaço, G., 2006. Estudo de caso da região do Sado: zonas costeiras. In: Santos, F.D., Miranda, P. Lisboa (Eds.), Alterações Climáticas em Portugal Cenários, Impactos e Medidas de Adaptação. p. 506. https://projects.eionet.europa.eu/2018-eea-report-national-cciv-assessments/library/national-documents/portugal/cap10-estudo-de-caso-da-regiao-do-sado/download/en/1/CAP10-Estudo%20de%20Caso%20da%20Regiao%20do%20Sado.pdf.

Andrew, M.E., Wulder, M.A., Nelson, T.A., 2014. Potential contributions of remote sensing to ecosystem service assessments. Prog. Phys. Geogr. Earth Environ. 38 (3). https://doi.org/10.1177/0309133314528942.

Aplin, P., 2006. On scales and dynamics in observing the environment. Int. J. Rem. Sens. 27, 2123–2140. https://doi.org/10.1080/01431160500396477.

Aroma, R.J., Raimond, K., 2016. An overview of technological revolution in satellite image analysis. Journal of Engineering Science and Technology Review 9 (4). Available in. https://fs.unm.edu/neut/AnOverviewOfTechnological.pdf.

Asmus, H., Asmus, R., 2000. Material exchange and food web of seagrass beds in the Sylt-Romo Bight: how significant are community changes at the ecosystem level? Helgoland Marine Research. BioMed Central 137–150. https://doi.org/10.1007/s101520050012.

Banerjee, B.P., Raval, S., 2022. Mapping sensitive vegetation communities in mining eco-space using UAV-LiDAR. Int J Coal Sci Technol 9, 40. https://doi.org/10.1007/s40789-022-00509-w.

Barillé, L., Mouget, J.L., Méléder, V., Rosa, P., Jesus, B., 2011. Spectral response of benthic diatoms with different sediment backgrounds. Remote Sens. Environ. 115, 1034–1042. https://doi.org/10.1016/j.rse.2010.12.008.

Barbosa, C.C.A., Atkinson, P.M., Dearing, J.A., 2015. Remote sensing of ecosystem services: a systematic review. Ecol. Indicat. 52, 430–443. https://doi.org/10.1016/j.ecolind.2015.01.007.

Bateman, I.J., Mace, G.M., Fezzi, C., Atkinson, G., Turner, K., 2011. Economic analysis for ecosystem service assessments. Environ. Resour. Econ. 48, 177–218. https://doi.org/10.1007/s10640-010-9418-x.

Bertels, L., Houthuys, R., Sterckx, S., Knaeps, E., Deronde, B., 2011. Large-scale mapping of the riverbanks, mud flats and salt marshes of the Scheldt basin, using airborne imaging spectroscopy and LiDAR. Int. J. Rem. Sens. 32, 2905–2918. https://doi.org/10.1080/01431161003745632.

Biguino, B., Sousa, F., Brito, A.C., 2021. Variability of Currents and Water Column Structure in a Temperate Estuarine System (Sado Estuary, Portugal). Water (Switzerland), vol. 13. https://doi.org/10.3390/w13020187.
Blaschke, T., Hay, G.J., Kelly, M., Lang, S., Hofmann, P., Addink, E., Queiroz Feitosa, R., van der Meer, F., van der Werff, H., van Coillie, F., Tiede, D., 2014. Geographic object-based image analysis - towards a new paradigm. ISPRS J. Photogrammetry Remote Sens. 87, 180–191. https://doi.org/10.1016/j.isprsjprs.2013.09.014.
Boyd, D.S., Sanchez-Hernandez, C., Foody, G.M., 2006. Mapping a specific class for priority habitats monitoring from satellite sensor data. Int. J. Rem. Sens. 27, 2631–2644. https://doi.org/10.1080/01431160600554348.
Brito, P.J.O., 2009. Impactos da elevação do nivel médio do mar em ambientes costeiros: o caso do estuário do Sado. PhD Thesis. University of Lisbon. Available in: http://hdl.handle.net/10451/3151.
Brito, A.C., Benyoucef, I., Jesus, B., Brotas, V., Gernez, P., Mendes, C.R., Launeau, P., Dias, M.P., Barillé, L., 2013. Seasonality of microphytobenthos revealed by remote-sensing in a South European estuary. Continent. Shelf Res. 66, 83–91. https://doi.org/10.1016/j.csr.2013.07.004.
Burgman, M.A., Lindenmayer, D.B., Elith, J., 2005. Managing landscapes for conservation under uncertainty. Ecology 86, 2007–2017. https://doi.org/10.1890/04-0906.
Calleja, F., Ondiviela, B., Galván, C., Recio, M., Juanes, J.A., 2019. Mapping estuarine vegetation using satellite imagery: the case of the invasive species Baccharis halimifolia at a Natura 2000 site. Continent. Shelf Res. 174, 35–47. https://doi.org/10.1016/j.csr.2019.01.002.
Casal, G., Sánchez-Carnero, N., Sánchez-Rodríguez, E., Freire, J., 2011. Remote sensing with SPOT-4 for mapping kelp forests in turbid waters on the south European Atlantic shelf. Estuar. Coast Shelf Sci. 91, 371–378. https://doi.org/10.1016/j.ecss.2010.10.024.
Castro, M.O.C.S.G., 1997. Comportamento dos PCBs e DDTs no Estuário do Sado e Bioacumulação em Peixes. U. T. L./I. S. T.
Chen, G., Jin, R., Ye, Z., Li, Q., Gu, J., Luo, M., Luo, Y., Christakos, G., Morris, J., He, J., Li, D., Wang, H., Song, L., Wang, Q., Wu, J., 2022. Spatiotemporal mapping of salt marshes in the intertidal zone of China during 1985-2019. J. Remote Sens. 2022. https://doi.org/10.34133/2022/9793626.
Conceição, R., 2016. Gestão de Dragagens Portuárias—Alguns Aspectos Geotécnicos e Geoambientais. Faculdade de Ciências e Tecnologia. Universidade Nova de Lisboa.
Congalton, R.G., 1991. A review of assessing the accuracy of classifications of remotely sensed data. Remote Sens. Environ. 37, 35–46.
Constanza, R., D'Arge, R., de Groot, R., Farber, S., Grasso, M., Hannon, B., Limburg, K., Naeem, S., O'Neill, R.V., Paruelo, J., Raskin, R.G., Sutton, P., van den Belt, M., 1997. The value of the world's ecosystem services and natural capital. Nature 387, 253–260. https://doi.org/10.1038/387253a0.
Cooley, S.W., Smith, L.C., Stepan, L., Mascaro, J., 2017. Tracking dynamic northern surface water changes with high-frequency Planet CubeSat imagery. Rem. Sens. 9, 1306. https://doi.org/10.3390/rs9121306.
Corbane, C., Lang, S., Pipkins, K., Alleaume, S., Deshayes, M., Millán, V.E.G., Strasser, T., Borre, J.V., Toon, S., Michael, F., 2015. Remote sensing for mapping natural habitats and their conservation status – new opportunities and challenges. Int. J. Appl. Earth Obs. Geoinf. 37, 7–16. https://doi.org/10.1016/j.jag.2014.11.005.
Coutinho, M.T.C.P., 2003. Comunidade Fitoplantónica do Estuário do Sado: Estrutura, dinâmica e aspectos ecológicos. INSTITUTO NACIONAL DE INVESTIGAÇÃO AGRÁRIA E DAS PESCAS - IPIMAR.
Cushnie, J.L., 1987. The interactive effect of spatial resolution and degree of internal variability within land-cover types on classification accuracies. Int. J. Rem. Sens. 8, 15–29.
Dalponte, M., Bruzzone, L., Vescovo, L., Gianelle, D., 2009. The role of spectral resolution and classifier complexity in the analysis of hyperspectral images of forest areas. Remote Sens. Environ. 113, 2345–2355. https://doi.org/10.1016/j.rse.2009.06.013.
Dash, J., Ogutu, B.O., 2016. Recent advances in space-born optical remote sensing systems for monitoring global terrestrial ecosystems. Prog. Phys. Geogr. 40, 322–351. https://doi.org/10.1177/0309133316639403.
Dixon, B., Candade, N., 2008. Multispectral landuse classification using neural networks and support vector machines: one or the other, or both? Int. J. Rem. Sens. 29, 1185–1206. https://doi.org/10.1080/01431160701294661.
Dronova, I., Kislik, C., Dinh, Z., Kelly, M., 2021. A review of unoccupied aerial Vehicle use in wetland applications: emerging opportunities in approach, technology, and data. Drones 5 (2), 45. https://doi.org/10.3390/drones5020045.
Edwards, T.C., Moisen, G.G., Cutler, D.R., 1998. Assessing map accuracy in a remotely sensed, ecoregion-scale cover map. Remote Sens. Environ. 63, 73–83. https://doi.org/10.1016/S0034-4257(96)00246-5.
Estes, J., Belward, A., Loveland, T., Scepan, J., Strahler, A., Townshend, J., Justice, C., 1999. The way forward. Photogramm. Eng. Rem. Sens. 65, 1089–1093.
EUNIS, 2012. EUNIS habitat classification 2012 [WWW Document]. URL. https://eunis.eea.europa.eu/habitats-code-browser.jsp. 11.22.22.
Feio, M.J., Ferreira, V., 2019. Rios de Portugal: comunidades, processos e alterações, Rios de Portugal: comunidades, processos e alterações. https://doi.org/10.14195/978-989-26-1624-7.
Feld, C.K., Sousa, J.P., da Silva, P.M., Dawson, T.P., 2010. Indicators for biodiversity and ecosystem services: towards an improved framework for ecosystems assessment. Biodivers. Conserv. 19, 2895–2919. https://doi.org/10.1007/s10531-010-9875-0.
Ferreira, J.G., Bettencourt, A., Bricker, S., Marques, J.C., Melo, J.J., Newton, A., Nobre, A., Patricio, J., Rocha, F., Rodrigues, R., Salas, F., Silva, M.C., Simas, J., Soares, C.V., Stacey, P.E., Vale, C., de Wit, M., Wolff, W.J., 2005. Monitoring plan for water quality and ecology of Portuguese transitional and coastal waters. INAG, IMAR. http://www.monae.org/documents/monae%20book.pdf.
Foley, J.A., DeFries, R., Asner, G.P., Barford, C., Bonan, G., Carpenter, S.R., Chapin, F.S., Coe, M.T., Daily, G.C., Gibbs, H.K., Helkowski, J.H., Holloway, T., Howard, E.A., Kucharik, C.J., Monfreda, C., Patz, J.A., Prentice, I.C., Ramankutty, N., Snyder, P.K., 2005. Global consequences of land use. Science 309 (5734), 570–574. https://doi.org/10.1126/science.1111772.
Foody, G.M., 2015. Valuing map validation: the need for rigorous land cover map accuracy assessment in economic valuations of ecosystem services. Ecol. Econ. 111, 23–28. https://doi.org/10.1016/j.ecolecon.2015.01.003.
Foody, G.M., 2010. Assessing the accuracy of land cover change with imperfect ground reference data. Remote Sens. Environ. 114, 2271–2285. https://doi.org/10.1016/j.rse.2010.05.003.
Foody, G.M., 2002. Status of land cover classification accuracy assessment. Remote Sens. Environ. 80, 185–201. https://doi.org/10.1016/S0034-4257(01)00295-4.
Frankenbach, S., Ezequiel, J., Plecha, S., Goessling, J.W., Vaz, L., Kühl, M., Dias, J.M., Vaz, N., Serôdio, J., 2020. Synoptic spatio-temporal variability of the photosynthetic productivity of microphytobenthos and phytoplankton in a tidal estuary. Front. Mar. Sci. 7, 170. https://doi.org/10.3389/fmars.2020.00170.
Ghuffar, S., 2018. DEM generation from multi satellite PlanetScope imagery. Rem. Sens. 10, 1462. https://doi.org/10.3390/rs10091462.
Gómez-Palacios, D., Torres, M.A., Reinoso, E., 2017. Flood mapping through principal component analysis of multitemporal satellite imagery considering the alteration of water spectral properties due to turbidity conditions. Geomatics, Nat. Hazards Risks 8, 607–623. https://doi.org/10.1080/19475705.2016.1250115.
Gong, P., Howarth, P.J., 1990. The use of structural information for improving land-cover classification accuracies at the rural-urban fringe. Photogramm. Eng. Rem. Sens. 56, 67–73.
Gray, P.C., Ridge, J.T., Poulin, S.K., Seymour, A.C., Schwantes, A.M., Swenson, J.J., Johnston, D.W., 2018. Integrating drone imagery into high resolution satellite remote sensing assessments of estuarine environments. Rem. Sens. 10, 1257. https://doi.org/10.3390/rs10081257.
Gupta, K., Mukhopadhyay, A., Giri, S., Chanda, A., Datta Majumdar, S., Samanta, S., Mitra, D., Samal, R.N., Pattnaik, A.K., Hazra, S., 2018. An index for discrimination of mangroves from non-mangroves using LANDSAT 8 OLI imagery. MethodsX 5, 1129–1139. https://doi.org/10.1016/j.mex.2018.09.011.
Gxokwe, S., Dube, T., Mazvimavi, D., 2022. Leveraging Google Earth Engine platform to characterize and map small seasonal wetlands in the semi-arid environments of South Africa. Sci. Total Environ. 803. https://doi.org/10.1016/j.scitotenv.2021.150139.
Haines-Young, R., Potschin, M., 2013. Common International Classification of Ecosystem Services (CICES): Consultation on Version 4, August - December 2012.
Haro, S., Jesus, B., Oiry, S., Papaspyrou, S., Lara, M., González, C.J., Corzo, A., 2022. Microphytobenthos spatio-temporal dynamics across an intertidal gradient using Random Forest classification and Sentinel-2 imagery. Sci. Total Environ. 804, 149983. https://doi.org/10.1016/j.scitotenv.2021.149983.
Haro, S., Lara, M., Laiz, I., González, C.J., Bohórquez, J., Garcia-Robledo, E., Corzo, A., Papaspyrou, S., 2020. Microbenthic net metabolism along intertidal gradients (cadiz bay, SW Spain): spatio-temporal patterns and environmental factors. Front. Mar. Sci. 7, 39. https://doi.org/10.3389/fmars.2020.00039.
Hawkins, D.M., Garrett, J.A., Stephenson, B., 2001. Some issues in resolution of diagnostic tests using an imperfect gold standard. Stat. Med. 20, 1987–2001. https://doi.org/10.1002/sim.819.
Hooper, T., Austen, M., 2020. Application of the Natural Capital Approach to Sustainability Appraisal: I) Final Report; 2) Method Summary.

Houborg, R., McCabe, M.F., 2016. High-resolution NDVI from Planet's Constellation of earth observation nano-satellites: a new data source for precision agriculture. Rem. Sens. 8, 768. https://doi.org/10.3390/rs8090768.
Hsieh, P.F., Lee, L.C., Chen, N.Y., 2001. Effect of spatial resolution on classification errors of pure and mixed pixels in remote sensing. IEEE Trans. Geosci. Rem. Sens. 39, 2657–2663.
Hunter, E.L., Power, C.H., 2002. An assessment of two classification methods for mapping Thames Estuary intertidal habitats using CASI data. Int. J. Rem. Sens. 23 (15), 2989–3008. https://doi.org/10.1080/01431160110075596.
ICNF, 2008. Plano Sectorial da Rede Natura 2000. Zonas de Proteção Especial. ZPE Estuário do Sado.
Iglseder, A., Immitzer, M., Dostálová, A., Kasper, A., Pfeifer, N., Bauerhansl, C., Schöttl, S., Hollaus, M., 2023. The potential of combining satellite and airborne remote sensing data for habitat classification and monitoring in forest landscapes. Int. J. Appl. Earth Obs. Geoinf. 117, 103131. https://doi.org/10.1016/j.jag.2022.103131.
Islam, M.A., Thenkabail, P.S., Kulawardhana, R.W., Alankara, R., Gunasinghe, S., Edussriya, C., Gunawardana, A., 2008. Semi-automated methods for mapping wetlands using Landsat ETM+ and SRTM data. Int. J. Rem. Sens. 29, 7077–7106. https://doi.org/10.1080/01431160802235878.
Jensen, J.R., 2006. Remote Sensing of the Environment: an Earth Resource Perspective, second ed. Pearson Prentice Hall, Upper Saddle River.
Jiao, L., Sun, W., Yang, G., Ren, G., Liu, Y., 2019. A hierarchical classification framework of satellite multispectral/hyperspectral images for mapping coastal wetlands. Rem. Sens. 11, 2238. https://doi.org/10.3390/rs11192238.
Katsanevakis, S., Stelzenmüller, V., South, A., Sørensen, T.K., Jones, P.J.S., Kerr, S., Badalamenti, F., Anagnostou, C., Breen, P., Chust, G., D'Anna, G., Duijn, M., Filatova, T., Fiorentino, F., Hulsman, H., Johnson, K., Karageorgis, A.P., Kröncke, I., Mirto, S., Pipitone, C., Portelli, S., Qiu, W., Reiss, H., Sakellariou, D., Salomidi, M., van Hoof, L., Vassilopoulou, V., Vega Fernández, T., Vöge, S., Weber, A., Zenetos, A., Hofstede, R., 2011. Ecosystem-based marine spatial management: review of concepts, policies, tools, and critical issues. Ocean Coast Manag. https://doi.org/10.1016/j.ocecoaman.2011.09.002.
Kennedy, R.E., Yang, Z., Cohen, W.B., Pfaff, E., Braaten, J., Nelson, P., 2012. Spatial and temporal patterns of forests disturbance and regrowth within the area of the northwest forest plan. Remote Sens. Environ. 122, 117–133. https://doi.org/10.1016/j.rse.2011.09.024.
Keramitsoglou, I., Sarimveis, H., Kiranoudis, C.T., Kontoes, C., Sifakis, N., Fitoka, E., 2006. The performance of pixel window algorithms in the classification of habitats using VHSR imagery. ISPRS J. Photogrammetry Remote Sens. 60, 225–238. https://doi.org/10.1016/j.isprsjprs.2006.01.002.
Knerr, S., Personnaz, L., Dreyfus, G., 1990. Single layer warning revisited a stepwise procedure for building and training a neural network, Neurocomputing: algorithms, architectures and applications. NATO ASI Series, Springer.
Koedsin, W., Intararuang, W., Ritchie, R.J., Huete, A., 2016. An integrated field and remote sensing method for mapping seagrass species, cover, and biomass in Southern Thailand. Rem. Sens. 8. https://doi.org/10.3390/rs8040292.
Koonsanit, K., Jaruskulchai, C., Eiumnoh, A., 2012. Band selection for dimension reduction in hyper spectral image using integrated information gain and principal components analysis technique. Int. J. Mach. Learn. Comput. 2, 248–251.
Krause, J.R., Oczkowski, A.J., Watson, E.B., 2023. Improved mapping of coastal salt marsh habitat change at Barnegat Bay (NJ, USA) using object-based image analysis of high-resolution aerial imagery. Remote Sens. Appl. Soc. Environ. 29. https://doi.org/10.1016/j.rsase.2022.100910.
Kromkamp, J.C., Morris, E.P., Forster, R.M., Honeywill, C., Hagerthey, S., Paterson, D.M., 2006. Relationship of intertidal surface sediment chlorophyll concentration to hyperspectral reflectance and chlorophyll fluorescence. Estuar. Coast 29, 183–196. https://doi.org/10.1007/BF02781988.
Li, C.H., Kuo, B.C., Lin, C.T., Huang, C.S., 2012. A spatial-contextual support vector machine for remotely sensed image classification. IEEE Trans. Geosci. Rem. Sens. 50, 784–799. https://doi.org/10.1109/TGRS.2011.2162246.
Li, J., Gao, S., Wang, Y., 2010. Invading cord grass vegetation changes analyzed from Landsat-TM imageries: a case study from the Wanggang area, Jiangsu coast, eastern China. Acta Oceanol. Sin. 29, 26–37. https://doi.org/10.1007/s13131-010-0034-y.
Liu, P., 2015. A survey of remote-sensing big data. Front. Environ. Sci. 3, 45. https://doi.org/10.3389/fenvs.2015.00045.
Lugendo, B., Wegoro, J., Shaghude, Y., Pamba, S., Makemie, M., Hollander, J., 2024. Seagrass mapping across the coast of Tanzania. Ocean Coast Manag. 253, 107169. https://doi.org/10.1016/j.ocecoaman.2024.107169.
Lyons, M.B., Keith, D.A., Phinn, S.R., Mason, T.J., Elith, J., 2018. A comparison of resampling methods for remote sensing classification and accuracy assessment. Remote Sens. Environ. 208, 145–153. https://doi.org/10.1016/j.rse.2018.02.026.
Mace, G.M., Hails, R.S., Cryle, P., Harlow, J., Clarke, S.J., 2015. Towards a risk register for natural capital. J. Appl. Ecol. 52, 641–653.
Madden, M., Jordan, T., Bernardes, S., Cotten, D.L., O'Hare, N., Pasqua, A., 2015. Unmanned aerial systems and structure from motion revolutionize wetlands mapping. In: Tiner, R.W., Lang, M.W., Klemas, V.V. (Eds.), Remote Sensing of Wetlands: Applications and Advances. CRC Press, USA, pp. 195–219.
Mather, P.M., 1999. Computer Processing of Remotely Sensed Images. An Introduction. John Wiley & Sons, Chichester, UK.
McFeeters, S.K., 1996. The use of the Normalized Difference Water Index (NDWI) in the delineation of open water features. Int. J. Rem. Sens. 17, 1425–1432. https://doi.org/10.1080/01431169608948714.
MEA, 2005. Ecosystems and Human Well-Being: Synthesis, Island Press, Washington, DC, p. 137. Millenium Ecosystem Assessment.
Melo, R., Nogueira Mendes, R., 2022a. ORTOSado-2021 Mapeamento Digital Do Habitat Prioritário Sebas (Ervas Marinhas) Do Estuário Do Sado. Technical Report. MARE – FCUL, Lisbon.
Melo, R., Nogueira Mendes, R., 2022b. ORTOSado-2021. MARE – FCUL, Lisbon. https://sigservices.icnf.pt/server/rest/services/BDG/pradarias_marinhas_sado/MapServer.
Morisette, J.T., Khorram, S., 2000. Accuracy-assessment curves for satellite-based change detection. Photogramm. Eng. Rem. Sens. 66, 875–880.
Mountrakis, G., Im, J., Ogole, C., 2011. Support vector machines in remote sensing: a review. ISPRS J. Photogrammetry Remote Sens. https://doi.org/10.1016/j.isprsjprs.2010.11.001.
Murray, N.J., 2018. Satellite remote sensing for the conservation of east asia's coastal wetlands. In: Leidner, A.K., Buchanan, G.M. (Eds.), Satellite Remote Sensing for Conservation Action: Case Studies from Aquatic and Terrestrial Ecosystems. Cambridge University Press, Cambridge, UK, pp. 54–81. https://doi.org/10.1017/9781108631129.
Murray, N.J., Keith, D.A., Bland, L.M., Ferrari, R., Lyons, M.B., Lucas, R., Pettorelli, N., Nicholson, E., 2018. The role of satellite remote sensing in structured ecosystem risk assessments. Sci. Total Environ. https://doi.org/10.1016/j.scitotenv.2017.11.034.
Najjar, A., Kaneko, S., Miyanaga, Y., 2017. Combining satellite imagery and open data to map road safety. Proc. - 31st AAAI Conf. Artif. Intell. 31. https://doi.org/10.1609/aaai.v31i1.11168.
Nunes, R.A.O., Alvim-Ferraz, M.C.M., Martins, F.G., Sousa, S.I.V., 2019. Environmental and social valuation of shipping emissions on four ports of Portugal. J. Environ. Manag. 235, 62–69. https://doi.org/10.1016/j.jenvman.2019.01.039.
O'Higgins, T.G., Ferraro, S.P., Dantin, D.D., Jordan, S.J., Chintala, M.M., 2010. Habitat scale mapping of fisheries ecosystem service values in estuaries. Ecol. Soc. 15. https://doi.org/10.5751/ES-03585-150407.
Oiry, S., Barillé, L., 2021. Using sentinel-2 satellite imagery to develop microphytobenthos-based water quality indices in estuaries. Ecol. Indicat. 121, 107184. https://doi.org/10.1016/j.ecolind.2020.107184.
Oommen, T., Misra, D., Twarakavi, N.K.C., Prakash, A., Sahoo, B., Bandopadhyay, S., 2008. An objective analysis of support vector machine based classification for remote sensing. Math. Geosci. 40, 409–424. https://doi.org/10.1007/s11004-008-9156-6.
Ouyang, Z.T., Zhang, M.Q., Xie, X., Shen, Q., Guo, H.Q., Zhao, B., 2011. A comparison of pixel-based and object-oriented approaches to VHR imagery for mapping saltmarsh plants. Ecol. Inf. 6, 136–146. https://doi.org/10.1016/j.ecoinf.2011.01.002.
Ozesmi, S.L., Bauer, M.E., 2002. Satellite remote sensing of wetlands. Wetl. Ecol. Manag. 10, 381–402. https://doi.org/10.1023/A:1020908432489.
Pal, M., Mather, P.M., 2005. Support vector machines for classification in remote sensing. Int. J. Rem. Sens. 26, 1007–1011. https://doi.org/10.1080/01431160512331314083.
Pe'eri, S., Morrison, J.R., Short, F., Mathieson, A., Lippmann, T., 2016. Eelgrass and macroalgal mapping to develop nutrient criteria in New Hampshire's estuaries using hyperspectral imagery. J. Coast Res. 76 (10076), 209–218. https://doi.org/10.2112/SI76-018.
Piaser, E., Villa, P., 2023. Evaluating capabilities of machine learning algorithms for aquatic vegetation classification in temperate wetlands using multi-temporal Sentinel-2 data. Int. J. Appl. Earth Obs. Geoinf. 117, 103202. https://doi.org/10.1016/j.jag.2023.103202.

Planet Team, 2017. Planet application program interface: in space for life on earth [WWW Document]. URL. https://api.planet.com. 11.17.22.
PlanetLabs, n.d. Planet Surface Reflectance Product v2 [WWW Document]. URL https://assets.planet.com/marketing/PDF/Planet_Surface_Reflectance_Technical_White_Paper.pdf (accessed 3.September.2023).
Poursanidis, D., Traganos, D., Reinartz, P., Chrysoulakis, N., 2019. On the use of Sentinel-2 for coastal habitat mapping and satellite-derived bathymetry estimation using downscaled coastal aerosol band. Int. J. Appl. Earth Obs. Geoinf. 80. https://doi.org/10.1016/j.jag.2019.03.012.
Qing, J., Huo, H., Fang, T., 2010. Supervised land cover classification based on the locally reduced convex hull approach. Int. J. Rem. Sens. 31, 2179–2187. https://doi.org/10.1080/01431161003636708.
Rainey, M.P., Tyler, A.N., Gilvear, D.J., Bryant, R.G., McDonald, P., 2003. Mapping intertidal estuarine sediment grain size distributions through airborne remote sensing. Remote Sens. Environ. 86, 480–490. https://doi.org/10.1016/S0034-4257(03)00126-3.
Randin, C., Ashcroft, M., Bolliger, J., Cavender-Bares, J., Coops, N., Dullinger, S., Dirnböck, T., Eckert, S., Ellis, E., Fernández, N., Giuliani, G., Guisan, A., Jetz, W., Joost, S., Karger, D.N., Lembrechts, J., Lenoir, J., Luoto, M., Morin, X., Payne, D., 2020. Monitoring biodiversity in the Anthropocene using remote sensing in species distribution models. Remote Sens. Environ. 239, 111626. https://doi.org/10.1016/j.rse.2019.111626.
Rocchini, D., Petras, V., Petrasova, A., Horning, N., Furtkevicova, L., Neteler, M., Leutner, B., Wegmann, M., 2017. Open data and open source for remote sensing training in ecology. Ecol. Inf. 40, 57–61. https://doi.org/10.1016/j.ecoinf.2017.05.004.
Rodarmel, C., Shan, C., 2002. Principal component analysis for hyperspectral image classification. Survey. Land Inf. Syst. 62, 115–123.
Roelfsema, C., Kovacs, E.M., Saunders, M.I., Phinn, S., Lyons, M., Maxwell, P., 2013. Challenges of remote sensing for quantifying changes in large complex seagrass environments. Estuar. Coast Shelf Sci. 133, 161–171. https://doi.org/10.1016/j.ecss.2013.08.026.
Samiappan, S., Turnage, G., Hathcock, L., Casagrande, L., Stinson, P., Moorhead, R., 2017. Using unmanned aerial vehicles for high-resolution remote sensing to map invasive Phragmites australis in coastal wetlands. Int. J. Rem. Sens. 38, 2199–2217. https://doi.org/10.1080/01431161.2016.1239288.
Santos, M., Amorim, A., Brotas, V., Cruz, J.P.C., Palma, C., Borges, C., Favareto, L.R., Veloso, V., Dâmaso-Rodrigues, M.L., Chainho, P., Félix, P.M., Brito, A.C., 2022. Spatio-temporal dynamics of phytoplankton community in a well-mixed temperate estuary (Sado Estuary, Portugal). Sci. Rep. 12, 1–18. https://doi.org/10.1038/s41598-022-20792-6.
Saul, S., Purkis, S., 2015. Semi-automated object-based classification of coral reef habitat using discrete choice models. Rem. Sens. 7, 15894–15916. https://doi.org/10.3390/rs71215810.
Sogno, P., Klein, I., Kuenzer, C., 2022. Remote sensing of surface water dynamics in the context of global change - a review. Rem. Sens. 14, 2475. https://doi.org/10.3390/rs14102475.
Sousa, M., 2006. Contribuição Para a Caracterização Geoambiental dos Sapais do Estuário do Sado—Aplicação Experimental no Ensino da Geologia. Faculdade de Ciências e Tecnologia, Universidade Nova de Lisboa.
Stehman, S.V., 2009. Sampling designs for accuracy assessment of land cover. Int. J. Rem. Sens. 30, 5243–5272. https://doi.org/10.1080/01431160903131000.
Stehman, S.V., 1997. Selecting and interpreting measures of thematic classification accuracy. Remote Sens. Environ. 62, 77–89. https://doi.org/10.1016/S0034-4257(97)00083-7.
Stratoulias, D., Balzter, H., Zlinszky, A., Tóth, V.R., 2018. A comparison of airborne hyperspectral-based classifications of emergent wetland vegetation at Lake Balaton, Hungary. Int. J. Rem. Sens. 39, 5689–5715. https://doi.org/10.1080/01431161.2018.1466081.
Sun, W., Liu, K., Ren, G., Liu, W., Yang, G., Meng, X., Peng, J., 2021. A simple and effective spectral-spatial method for mapping large-scale coastal wetlands using China ZY1-02D satellite hyperspectral images. Int. J. Appl. Earth Obs. Geoinf. 104, 102572. https://doi.org/10.1016/j.jag.2021.102572.
Tallis, H., Mooney, H., Andelman, S., Balvanera, P., Cramer, W., Karp, D., Polasky, S., Reyers, B., Ricketts, T., Running, S., Thonicke, K., Tietjen, B., Walz, A., 2012. A global system for monitoring ecosystem service change. Bioscience 62 (11), 977–986. https://doi.org/10.1525/bio.2012.62.11.7.
Thomson, A.G., Fuller, R.M., Yates, M.G., Brown, S.L., Cox, R., Wadsworth, R.A., 2003. The use of airborne remote sensing for extensive mapping of intertidal sediments and saltmarshes in eastern England. Int. J. Rem. Sens. 24, 2717–2737. https://doi.org/10.1080/0143116031000066918.
Tian, Y.Q., Yu, Q., Zimmerman, M.J., Flint, S., Waldron, M.C., 2010. Differentiating aquatic plant communities in a eutrophic river using hyperspectral and multispectral remote sensing. Freshw. Biol. 55, 1658–1673. https://doi.org/10.1111/j.1365-2427.2010.02400.x.
Timm, B.C., McGarigal, K., 2012. Fine-scale remotely-sensed cover mapping of coastal dune and salt marsh ecosystems at Cape Cod National Seashore using Random Forests. Remote Sens. Environ. 127, 106–117. https://doi.org/10.1016/j.rse.2012.08.033.
Tiner, R.W., 2015. Introducing to wetland mapping and its challenge. In: Tiner, R.W., Lang, M.W., Klemas, V.V. (Eds.), Remote Sensing of Wetlands: Applications and Advances. CRC Press, Taylor & Francis Group, pp. 43–66.
Traganos, D., Lee, C.B., Blume, A., Poursanidis, D., Čižmek, H., Deter, J., Mačić, V., Montefalcone, M., Pergent, G., Pergent-Martini, C., Ricart, A.M., Reinartz, P., 2022. Spatially explicit seagrass extent mapping across the entire mediterranean. Front. Mar. Sci. 9, 1276. https://doi.org/10.3389/fmars.2022.871799.
Traganos, D., Reinartz, P., 2018. Mapping mediterranean seagrasses with sentinel-2 imagery. Mar. Pollut. Bull. 134, 197–209. https://doi.org/10.1016/j.marpolbul.2017.06.075.
Traganos, D., Terauchi, G., Glavan, J., Panyawai, J., Creed, J., Wearherdon, L.V., McKenzie, L., Stankovic, M., Sagawa, T., Komatsu, T., Poursanidis, D., 2020. Seagrass mapping and monitoring. In: Out of the Value - the Value of Seagrasses to the Environment and to People. United Nations Environment Programme, UNEP, Nairobi.
Underwood, G.J.C., Kromkamp, J., 1999. Primary production by phytoplankton and microphytobenthos in estuaries. In: Advances in Ecological Research. Academic Press, pp. 93–153. https://doi.org/10.1016/S0065-2504(08)60192-0.
Vacek, P.M., 1985. The effect of conditional dependence on the evaluation of diagnostic tests. Biometrics 41, 959–968. https://doi.org/10.2307/2530967.
Valenstein, P.N., 1990. Evaluating diagnostic tests with imperfect standards. Am. J. Clin. Pathol. 93, 252–258. https://doi.org/10.1093/ajcp/93.2.252.
Valentini, E., Taramelli, A., Filipponi, F., Giulio, S., 2015. An effective procedure for EUNIS and Natura 2000 habitat type mapping in estuarine ecosystems integrating ecological knowledge and remote sensing analysis. Ocean Coast Manag. 108, 52–64. https://doi.org/10.1016/j.ocecoaman.2014.07.015.
van der Wal, D., van Dalen, J., den Dool, A.W., Dijkstra, J.T., Ysebaert, T., 2014. Biophysical control of intertidal benthic macroalgae revealed by high-frequency multispectral camera images. J. Sea Res. 90, 111–120. https://doi.org/10.1016/j.seares.2014.03.009.
van Maren, D.S., van Kessel, T., Cronin, K., Sittoni, L., 2015. The impact of channel deepening and dredging on estuarine sediment concentration. Continent. Shelf Res. 95, 1–14. https://doi.org/10.1016/j.csr.2014.12.010.
Vapnik, V., 1995. The Nature of Statistical Learning Theory. Springer-Verlag, New York, USA.
Wang, Y., Yésou, H., 2018. Remote sensing of floodpath lakes and wetlands: a challenging frontier in the monitoring of changing environments. Rem. Sens. 10, 1955. https://doi.org/10.3390/RS10121955.
Wang, X., Gao, X., Zhang, Y., Fei, X., Chen, Z., Wang, J., Zhang, Y., Lu, X., Zhao, H., 2019. Land-cover classification of coastal wetlands using the RF algorithm for worldview-2 and landsat 8 images. Rem. Sens. 11 (16), 1927. https://doi.org/10.3390/rs11161927.
Wang, Y., Jin, S., Dardanelli, G., 2024. Vegetation classification and evaluation of yancheng coastal wetlands based on random forest algorithm from sentinel-2 images. Rem. Sens. 16 (7), 1124. https://doi.org/10.3390/rs16071124.
Weires, S., Bock, M., Wissen, M., Rossner, G., 2004. Mapping and indicator approaches for the assessment of habitats at different scales using remote sensing and GIS methods. Landsc. Urban Plann. 67, 43–65. https://doi.org/10.1016/S0169-2046(03)00028-8.
Wicaksono, P., Lazuardi, W., 2018. Assessment of PlanetScope images for benthic habitat and seagrass species mapping in a complex optically shallow water environment. Int. J. Rem. Sens. 39, 5739–5765. https://doi.org/10.1080/01431161.2018.1506951.
Wulder, M.A., Masek, J.G., Cohen, W.B., Loveland, T.R., Woodcock, C.E., 2012. Opening the archive: how free data has enabled the science and monitoring promise of Landsat. Remote Sens. Environ. 122, 2–10. https://doi.org/10.1016/j.rse.2012.01.010.
Xie, Y., Sha, Z., Yu, M., 2008. Remote sensing imagery in vegetation mapping: a review. J. Plant Ecol. 1 (1), 9–23. https://doi.org/10.1093/jpe/rtm005.
Xu, H., 2006. Modification of normalised difference water index (NDWI) to enhance open water features in remotely sensed imagery. Int. J. Rem. Sens. 27, 3025–3033. https://doi.org/10.1080/01431160600589179.
Yu, M., Li, Y., Zhang, K., Yu, J., Guo, X., Guan, B., Yang, J., Zhou, D., Wang, X., Li, X., Zhang, X., 2023. Studies on the dynamic boundary of the fresh-salt water interaction zone of estuary wetland in the Yellow River Delta. Ecol. Eng. 188. https://doi.org/10.1016/j.ecoleng.2023.106893.
Zhang, C., 2015. Applying data fusion techniques for benthic habitat mapping and monitoring in a coral reef ecosystem. ISPRS J. Photogrammetry Remote Sens. 104,

213–223. https://doi.org/10.1016/j.isprsjprs.2014.06.005.
Zhang, Y., Lu, D., Yang, B., Sun, C., Sun, M., 2011. Coastal wetland vegetation classification with a Landsat thematic mapper image. Int. J. Rem. Sens. 32, 545–561. https://doi.org/10.1080/01431160903475241.
Zhong, Y., Zhang, L., Gong, J., Li, P., 2007. A supervised artificial immune classifier for remote-sensing imagery. In: IEEE Transactions on Geoscience and Remote Sensing. pp. 3957–3966. https://doi.org/10.1109/TGRS.2007.907739.
Zhou, W., Guan, H., Li, Z., Shao, Z., Delavar, M.R., 2023. Remote sensing image retrieval in the past decade: achievements, challenges, and future directions. IEEE J. Sel. Top. Appl. Earth Obs. Rem. Sens. 16, 1447–1473. https://doi.org/10.1109/JSTARS.2023.3236662.